Kornerupine at the Sar-e-Sang, Afghanistan, whiteschist locality: Implications for tourmaline-kornerupine distribution in metamorphic rocks

Edward S. Grew

Department of Geological Sciences, University of Maine, Orono, Maine 04469, U.S.A.

Abstract

In the upper-amphibolite rocks at Sar-e-Sang (northeastern Afghanistan), tourmaline is the characteristic accessory borosilicate in the whiteschists (talc-kyanite rocks), whereas kornerupine has been reported in a magnesite-phlogopite rock.

A specimen of the Sar-e-Sang kornerupine-bearing rock also contains trace amounts of enstatite, sapphirine, forsterite, and spinel. Enstatite is in contact with magnesite and sapphirine is nearly so, whereas forsterite is entirely enclosed in kornerupine.

Electron- and ion-microprobe analyses yield the following formulae (idealized anion content): average magnesite, $Mg_{1.97}Ca_{0.02}Fe_{0.01}(CO_3)$; a sapphirine, $Mg_{3.78}Fe_{0.03}B_{0.02}Al_{8.41}Si_{1.77}O_{20}$; an enstatite, $Mg_{1.92}Fe_{0.02}Al_{0.13}Si_{1.93}O_6$; average phlogopite, $(K_{1.39}Na_{0.50})(Mg_{5.53}Fe_{0.03}Al_{0.45}Ti_{0.01})(Al_{2.39}Si_{5.61}O_{20})(OH)_{3.73}F_{0.27}$; kornerupines, $(Ca_{0.02}Na_{0.01})(Mg_{3.81}Fe_{0.03}Mn_{0.01}Li_{0.03}Al_{5.50})(Si_{3.70}Al_{0.92}B_{0.38})O_{21}(OH)_{0.97}F_{0.03}$ and $(Ca_{0.01}Na_{0.01})(Mg_{4.06}Fe_{0.03}Li_{0.01}Al_{5.31})(Si_{3.84}Al_{0.51}B_{0.65})O_{21}(OH)_{0.97}F_{0.03}$; average forsterite, $(Mg_{1.97}Fe_{0.02})SiO_4$; and average spinel, $(Mg_{0.98}Fe_{0.03})Al_{1.99}O_4$.

The bulk composition of the kornerupine-bearing rock is SiO_2 29.7%, Al_2O_3 18.9%, B_2O_3 0.55%, Fe as Fe_2O_3 0.31%, MnO 0.027%, MgO 29.6%, CaO 0.23%, Na_2O 0.72%, K_2O 3.5%, Li_2O 0.018%, F 0.25%, loss on ignition 16.5%, moisture 0.31%, and total 100.62 wt%. The precursor was probably an argillaceous sedimentary rock associated with evaporites, and the variable B content in kornerupine could reflect heterogeneous distribution of B in this sedimentary rock.

Conditions of metamorphism are estimated, by comparison with experimental results and theoretical calculations, to be ≥ 7 kbar and 630–670 °C and $X_{CO_2} \geq 0.15$ (fluid phase) for the kornerupine + phlogopite + magnesite ± sapphirine ± enstatite assemblage, which formed under the same pressure-temperature conditions as the kyanite + talc + tourmaline (± gedrite) assemblages described by W. Schreyer and K. Abraham in the associated whiteschists. A μ_{CO_2}-μ_{H_2O} diagram for the major phases in the kornerupine-bearing rock and whiteschist suggests that the kornerupine-bearing rock crystallized at a higher μ_{CO_2} and lower μ_{H_2O} than the tourmaline-bearing whiteschists. Nonetheless, the main control on kornerupine and tourmaline distribution appears to have been the whole-rock SiO_2 content. The activities of CO_2 and H_2O were partially buffered by the mineral parageneses of the rocks so that gradients developed, although CO_2 and H_2O appear to have been fully mobile components. The breakdown of tourmaline to kornerupine is predicted to have been a hydration reaction in the Sar-e-Sang rocks. As a result, kornerupine-tourmaline relations in the Sar-e-Sang rocks differ from those expected in the chemically more complex metapelites, in which these breakdown reactions are probably dehydration reactions and are in part controlled by metamorphic fluids or anatectic melts.

Introduction

A commonly observed feature of metapelitic rocks is the disappearance of tourmaline under upper amphibolite–facies conditions. At lower grades, tourmaline is a nearly ubiquitous accessory in metapelites (e.g., Henry and Guidotti, 1985), whereas in the granulite-facies, it is rare. The disappearance of tourmaline is particularly surprising in view of its persistence to high temperatures in laboratory experiments (e.g., 850 °C at 2 kbar, Robbins

and Yoder, 1962; 790 °C at 1 kbar, Pichavant and Manning, 1984).

In most cases, tourmaline disappears from the rock altogether. In a few granulite-facies pelitic rocks or rocks similar to pelite but enriched in Mg and Al, the borosilicates grandidierite or kornerupine appear together with tourmaline (e.g., Girault, 1952; Grew and Hinthorne, 1983; Waters and Moore, 1985; Grew, 1986, 1987). Study of rocks with two or more borosilicate minerals may clarify the reactions defining the limits of tourmaline stabil-

ity. However, pelitic rocks are chemically complex. Anatexis and other processes associated with migmatization play an important role in their evolution under upper amphibolite–facies and granulite-facies conditions. An alternative approach is to study the parageneses of borosilicates in rocks that are chemically simpler than pelites and that are not migmatized. The whiteschists (talckyanite rocks, Schreyer, 1973) and associated rocks at the Sar-e-Sang lapis-lazuli deposit in northeastern Afganistan provide such an opportunity.

Tourmaline is a common accessory in the whiteschists (Kulke and Schreyer, 1973; Schreyer and Abraham, 1976), whereas kornerupine is a major constituent in a magnesite-phlogopite rock (Blaise and Cesbron, 1966) from the same locality. Both the tourmaline-bearing whiteschist and the kornerupine-bearing rock are highly magnesian metasedimentary rocks, the chemistry of which is readily modeled by a relatively simple chemical system. In the present paper, I report the results of my detailed investigation on a piece of Blaise and Cesbron's (1966) kornerupine-bearing rock obtained from F. Cesbron. By comparing this rock with the tourmaline-bearing whiteschists that Schreyer and Abraham (1975, 1976) studied in detail, I attempt to define the physico-chemical controls on the distribution of tourmaline and kornerupine at Sar-e-Sang, and I also consider the implications of my study for kornerupine-tourmaline distribution in general.

GEOLOGIC BACKGROUND

Sar-e-Sang and nearby areas are largely underlain by sillimanite ± kyanite + garnet ± cordierite gneiss, amphibole gneiss, amphibolite, calc-silicate rocks, and dolomitic marble metamorphosed under upper amphibolite–facies conditions (muscovite and orthopyroxene are absent, Blaise and Cesbron, 1966; Yefimov and Sudderkin, 1967; Yurgenson and Sukharev, 1984). Other rocks reported by these authors from Sar-e-Sang and nearby areas include quartzite, pyroxenite (augite + hornblende + plagioclase), and peridotite. The age of these metamorphic rocks is generally considered to be Precambrian (e.g., Blaise and Cesbron, 1966), but Kulke and Schreyer (1973) suggested that the metamorphism could also be Caledonian. In general, the layers at Sar-e-Sang trend north-south and dip steeply east (Blaise and Cesbron, 1966).

The kornerupine-bearing rock, as well as the whiteschists (Kulke and Schreyer, 1973), is reported to be found near the base of a marble unit, several hundreds of meters thick, whereas the deposits of lapis lazuli occur toward the center of this unit. The marble + calc-silicate unit structurally overlies a sillimanite + garnet gneiss. Blaise and Cesbron (1966) reported that lenses of quartz + albite (Ab_{90}–Ab_{95}) rock exposed immediately under the marble + calc-silicate unit contain accessory tourmaline, in places in sufficient abundance to be called a tourmalinite. Blaise and Cesbron (1966) attributed the quartz + albite + tourmaline rock, pegmatites, and veins of granitic composition to a postmetamorphic period of re-

gional migmatization and granitization. Yurgenson and Sukharev (1984) reported that tourmaline-bearing granite and other quartzofeldspathic rocks are closely associated with the lapis lazuli, including a quartz + K-feldspar + albite rock with clinopyroxene, amphiboles, tourmaline, phlogopite, pyrite, and accessories.

Blaise and Cesbron (1966) and Yurgenson and Sukharev (1984) proposed a metasomatic origin for the lapis lazuli on the basis of D. S. Korzhinskiy's (1947) pioneering work on Baikal lapis deposits. In brief, the lapis lazuli is interpreted to have formed through high-temperature metasomatic exchange between quartzofeldspathic rocks (either plutonic or metasedimentary in origin) and marble in the presence of sodic solutions produced by anatectic processes. Pyrite in the marble and in associated calc-silicate rocks and metasomatites is believed to be the source of S for lazurite and associated hauyne and sodalite. An alternative interpretation was proposed by Kulke (1976) and Schreyer and Abraham (1976). On the basis of relict anhydrite and gypsum rocks, these authors proposed that the lapis lazuli and whiteschists are parts of a metamorphosed evaporite deposit that was extensively modified by melting and volatilization. Metasomatism is not needed to explain the formation of lapis lazuli. The highly magnesian compositions and elevated B contents of the whiteschists are characteristic of argillites associated with evaporites (Moine et al., 1981). The tourmaline-rich albitic rocks reported by Blaise and Cesbron (1966) may also represent premetamorphic B enrichment, such as the submarine exhalative process Plimer (1983) proposed for similar tourmaline + albite rocks at Broken Hill, Australia.

The whiteschists described by Kulke and Schreyer (1973) and Schreyer and Abraham (1976) and the kornerupine-bearing rock described by Blaise and Cesbron (1966) may have been collected within a few meters or tens of meters of each other. Moreover, given Blaise and Cesbron's (1966) report of no evidence for a granite massif in the vicinity of the Sar-e-Sang deposit, there is no reason to expect significant gradients in metamorphic temperatures and pressures. Thus, both rock types crystallized under the same pressure-temperature conditions over the entire course of their metamorphic history. The distribution of tourmaline and kornerupine evidently was not the result of variations in pressure and temperature but of other factors, either whole-rock compositions or chemical potentials of the mobile components.

PETROGRAPHIC DESCRIPTION

The fragment (originally 4 × 2 × 2 cm across) of Cesbron's specimen (no. 12-84-17) made available to me is a white, fine- to medium-grained (0.05–1.4 mm), somewhat splintery rock with a distinct foliation and lineation resulting from the preferred orientation of colorless phlogopite. Blaise and Cesbron (1966) reported that this rock originated from a concordant layer or vein in marble. The single thin section examined and used for microprobe analysis was cut perpendicular to the lineation.
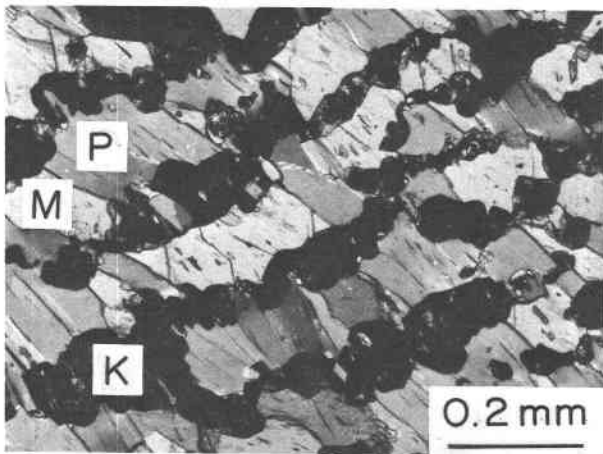
Fig. 1. Photomicrograph of a kornerupine-magnesite patch in the Sar-e-Sang kornerupine rock. In these patches, kornerupine grains form lamellae (K, black) at a high angle to phlogopite (P) foliation (upper left to lower right in photo). M = Magnesite. Crossed nicols.
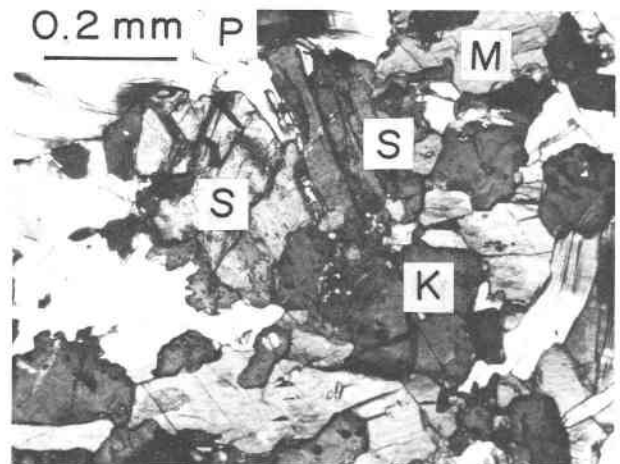

Fig. 2. Photomicrograph of Sar-e-Sang kornerupine-bearing rock. Sapphirine (S) (analysis 1, Fig. 5) is largely enclosed in kornerupine (K), but touches phlogopite (P) and almost touches magnesite (M). Crossed nicols.

Kornerupine (mostly 0.05–1 mm and thereby finer grained than phlogopite and magnesite) and magnesite form irregular patches of symplectite in which the kornerupine grains are arranged as parallel lamellae in magnesite aggregates, generally with phlogopite; Figure 1 shows a portion of one such patch (cf. Fig. 5, Blaise and Cesbron, 1966). Phlogopite is the dominant mineral between these patches. An estimate of the mode based on 2900 counts is 51.4 vol% phlogopite, 27.9% magnesite, and 20.7% kornerupine. Minerals not reported by Blaise and Cesbron (1966), namely sapphirine, enstatite, spinel, and forsterite, occur only in trace amounts. The first three minerals occur only over a 5 × 6 mm area in the thin section. Sapphirine forms tabular to equant grains almost entirely enclosed in kornerupine but locally in contact with phlogopite and in one place, almost in contact with magnesite (Fig. 2). Enstatite, which is locally replaced by talc (?) or anthophyllite (?), is in contact with magnesite and phlogopite (Fig. 3). Enstatite also appears to have been in contact with kornerupine, but the later alteration of enstatite has largely obscured the few grain contacts found between the two minerals. The single forsterite grain is isolated from the other minerals by an aggregate of kornerupine on one side (Fig. 4); the other side is on the edge of the section. This is the first report, as far as I am aware, of a natural forsterite-kornerupine assemblage. This assemblage has not been reported in laboratory syntheses (Seifert, 1975; Werding and Schreyer, 1978). A few grains of spinel occur in contact with magnesite and phlogopite about 1.5 cm from the nearest enstatite and sapphirine and in a second patch more than 2 cm distant.

The intergrowth of magnesite, kornerupine, and phlogopite is interpreted to result from coeval crystallization, and the relations described above suggest that sapphirine is in textural equilibrium with these three phases. Enstatite does not touch sapphirine, but the closest approach

of enstatite to sapphirine (0.15 mm) suggests that enstatite probably equilibrated with it. Thus the equilibrium assemblage for the 5 × 6 mm area is kornerupine + phlogopite + magnesite + enstatite + sapphirine (Fig. 5).

Spinel occurs no closer than 1.5 cm distant from sapphirine and enstatite, whereas forsterite is isolated from the other major components by kornerupine. Thus spinel and forsterite may not have equilibrated with the sapphirine + enstatite + kornerupine + magnesite + phlogopite assemblage in the 5 × 6 mm patch. The addition of either spinel or forsterite to this assemblage would violate the phase rule in the $MgO-Al_2O_3-SiO_2-B_2O_3-CO_2-H_2O$ system if CO_2 and H_2O are assumed to be fully mobile components in the sense of Korzhinskiy (1957, 1973).
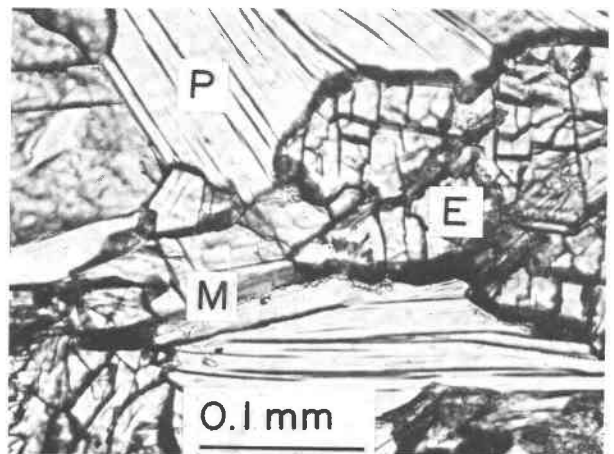

Fig. 3. Photomicrograph of Sar-e-Sang kornerupine-bearing rock with enstatite (E) in contact with magnesite (M) and phlogopite (P). Plane-polarized light.
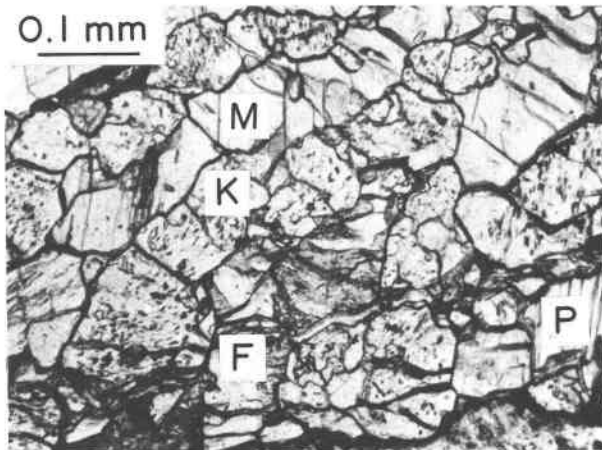
Fig. 4. Photomicrograph of forsterite (F) in the Sar-e-Sang kornerupine-bearing rock. Kornerupine (K) surrounds and isolates forsterite from magnesite (M). P = Phlogopite. One end of forsterite grain is broken by edge of the section (bottom of photograph). Plane-polarized light.

Fig. 5. Plot (in molecular proportions) of Sar-e-Sang whiteschist (SSg42) and kornerupine-bearing rock (12-84-17) (filled squares) and mineral compositions (filled circles) projected through (K,Na)-phlogopite into the tetrahedron (Mg,Fe)O-Al$_2$O$_3$-SiO$_2$-B$_2$O$_3$ (B$_2$O$_3$ apex can be visualized as lying below the triangle). Observed mineral compatibilities are indicated by solid lines (for second stage only in the whiteschist; Schreyer and Abraham, 1976), and the dashed line indicates a possible Ged-Tur-Spr assemblage.

However, a local spinel + kornerupine + magnesite + phlogopite assemblage (Fig. 5) is possible in silica-poor patches, assuming "mosaic equilibrium" (see below). On the other hand, a local forsterite + enstatite + magnesite assemblage is not indicated by the textural relations because forsterite is armored by kornerupine. For the purposes of discussion, I will assume that forsterite is not part of the mineral assemblage in the 5 × 6 mm area. Possibly forsterite is relict from the earlier stage of metamorphism. Under somewhat higher X_{H_2O} (lower X_{CO_2}) conditions, forsterite would be stable instead of magnesite + enstatite.

On the basis of Schreyer and Abraham's (1976) petrographic descriptions and discussions of mineral compatibilities in the whiteschists, the mineral compatibilities for their second stage of metamorphism (during which the kornerupine-bearing assemblage formed; see below) are interpreted to be kyanite + talc + tourmaline + phlogopite (SSg42) and kyanite + talc + gedrite + quartz + phlogopite (SSg42a) (Fig. 5). Moreover, judging from Kulke and Schreyer's (1973) discussion, I presume a tourmaline + gedrite + kyanite + talc assemblage may have also been stable during the second stage in other samples from this locality. Consequently, a tourmaline-gedrite join is included in Figure 5. Both tourmaline + talc and tourmaline + gedrite (with kyanite) appear only in the whiteschists, which have relatively high SiO$_2$ contents compared to Blaise and Cesbron's (1966) rock (Fig. 5).

Possible compatibilities at lower SiO$_2$ contents in the whiteschists are found only in the cordierite reaction rims developed between kyanite and gedrite during a later stage of metamorphism (the third stage of Schreyer and Abraham, 1976; see below). In SSg42a, Schreyer and Abraham (1976) described tourmaline in a cordierite reaction rim between kyanite and gedrite, but did not further specify
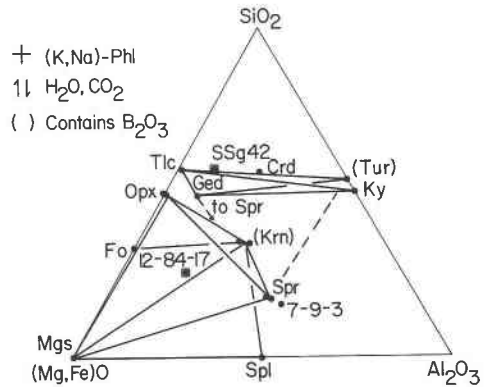
the assemblage. This tourmaline may have equilibrated with cordierite, gedrite, kyanite, sillimanite, sapphirine, or corundum. Grew et al. (1988) found tourmaline + cordierite + corundum ± kyanite assemblages in similar reaction rims in talc + kyanite + hornblende rocks from Kugi-Lal, southwestern Pamirs, USSR, about 120 km from Sar-e-Sang. Despite the absence of detailed information on the tourmaline assemblage in the Sar-e-Sang whiteschist, it is significant that tourmaline, and not kornerupine, appears in a silica-undersaturated portion of the whiteschist. This observation has important implications for interpreting the kornerupine-tourmaline distribution in the Sar-e-Sang rocks.

WHOLE-ROCK AND MINERAL CHEMISTRY

Methods

The composition of the rock was determined at Skyline Labs, Inc., in Denver, Colorado, under the direction of Gordon van Sickle, by inductively coupled Ar-plasma spectrometry (oxides), specific ion electrode (F), and gravimetry (loss on ignition, moisture).

The compositions of the minerals for elements other than Li, Be, B, F, and Ba were determined with the electron-microprobe analyzer (EMA). Most of the minerals were analyzed at the Ruhr-Universität Bochum using natural and synthetic compounds as standards (Grew et al., 1987), and data were reduced by the MISO program (Schreyer et al., 1984). Within the 5 × 6 mm area where sapphirine, enstatite, and forsterite appear, three to six grains of kornerupine, phlogopite, magnesite, enstatite, and sapphirine were analyzed at one to six points per grain. M. Yates analyzed the forsterite grain at six points and a spinel mass at 12 points with the MAC 400S electron microprobe (15 kV, 0.03-μA beam current) at the University of Maine in Orono, and the data were corrected using Bence and Albee factors. In addition, a grain each of forsterite, phlogopite, and sapphirine, and three grains of korne-

TABLE 1. Whole-rock composition, Sar-e-Sang kornerupine rock (in wt%)

SiO_2	29.7
Al_2O_3	18.9
Fe_2O_3	0.31
MnO	0.027
MgO	29.6
CaO	0.23
Na_2O	0.72
K_2O	3.5
Li_2O	0.018
B_2O_3	0.55
F	0.25
L.O.I.*	16.5
Moist.**	0.31
Total	100.62

Note: All Fe as Fe_2O_3. Analyzed at Skyline Labs, Inc., Denver, Colorado under direction of Gordon H. van Sickle. Sample no. 12-84-17.
* Loss on ignition at 1000 °C, probably mostly CO_2.
** Moisture at 105 °C.

rupine, were analyzed with the assistance of N. Marquez for Li, Be, B, F, and Ba with the ion-microprobe mass analyzer (IMMA) at the Aerospace Corporation in Los Angeles, California. The raw count data were processed by the working-curve approach described by Grew and Hinthorne (1983) and Grew et al. (1986).

Rock and mineral compositions

The kornerupine-bearing rock is remarkable for its high MgO and CO_2 contents and low total Fe and SiO_2 contents (Table 1, Fig. 5). Its high B/Al ratio (0.04) and contents of F (2500 ppm), K, and Mg suggest that the precursor could have been an argillaceous sedimentary rock associated with evaporites (Moine et al., 1981).

The component minerals have unusually low Fe contents, none of which exceed 1.25% FeO (spinel), and are consequently highly magnesian, with $100X_{Fe} = 100[Fe/(Fe + Mg)]_{atomic}$ ranging from 0.5 to 2.5 (Table 2).

TABLE 2. Selected analyses of minerals in Sar-e-Sang kornerupine rock

Grain:	Kornerupine* 1	Kornerupine* 2	Kornerupine* 3	Phlogopite* Average	Sapphirine 2	Orthopyroxene 1	Orthopyroxene 2	Forsterite 1	Spinel 1
				Electron microprobe (wt%)					
SiO_2	30.68	30.93	31.68	40.23	15.22	57.65	56.70	42.36	b.d.
TiO_2	0.04	b.d.	b.d.	0.06	b.d.	b.d.	0.04	0.01	0.03
Al_2O_3	45.26	42.38	40.71	17.26	61.32	1.96	3.15	0.09	70.80
Cr_2O_3	0.03	b.d.	b.d.	b.d.	b.d.	b.d.	b.d.	b.d.	b.d.
FeO	0.33	0.27	0.29	0.25	0.30	0.85	0.79	1.01	1.25
MnO	0.05	0.05	0.04	b.d.	b.d.	0.09	0.04	0.05	0.06
MgO	21.23	21.84	22.42	26.57	21.79	38.43	37.92	55.76	27.60
CaO	0.12	0.07	0.07	b.d.	b.d.	0.07	0.06	0.03	b.d.
Na_2O	0.04	0.04	0.03	1.83	b.d.	b.d.	b.d.	—	—
K_2O	b.d.	b.d.	b.d.	7.82	b.d.	b.d.	b.d.	—	—
				Ion microprobe (wt%)					
Li_2O	0.07	0.03	0.03	0.004	0.003	—	—	0.0005	—
B_2O_3	1.83	2.28	3.09	b.d.	0.08	—	—	0.03	—
F	0.08	0.07	0.07	0.60	b.d.	—	—	0.02	—
BaO	b.d.	b.d.	b.d.	0.08	b.d.	—	—	b.d.	—
				Calculated (wt%)					
H_2O	1.21	1.19	1.20	4.01	—	—	—	—	—
Total	100.94	99.12	99.60	98.46	98.71	99.05	98.62	99.36	99.74
				Cations and number of oxygens					
Oxygens	21.5	21.5	21.5	22	20	6	6	4	4
Si	3.695	3.785	3.844	5.613	1.771	1.955	1.930	1.002	0.000
Al	0.924	0.734	0.509	2.387	4.212	0.045	0.070	0.000	—
B	0.381	0.481	0.647	0.000	0.017	—	—	0.001	—
Total	5.000	5.000	5.000	8.000	6.000	2.000	2.000	1.003	0.000
Ti	0.004	0.000	0.000	0.006	0.000	0.000	—	0.000	0.001
Al	5.501	5.378	5.313	0.451	4.200	0.034	0.056	0.003	1.993
Cr	0.003	0.000	0.000	0.000	0.000	0.000	0.000	0.000	0.000
Fe	0.033	0.028	0.029	0.029	0.029	0.024	0.023	0.020	0.025
Mn	0.005	0.005	0.004	0.000	0.000	0.003	0.001	0.001	0.001
Mg	3.812	3.984	4.056	5.526	3.781	1.942	1.924	1.967	0.983
Li	0.033	0.016	0.013	0.002	0.001	—	—	0.000	—
Total	9.392	9.411	9.415	6.014	8.011	2.003	2.004	—	3.003
Ca	0.015	0.009	0.009	0.000	0.000	0.003	0.002	0.001	0.000
Na	0.009	0.009	0.007	0.495	0.000	0.000	0.000	—	—
K	0.000	0.000	0.000	1.392	0.000	0.000	0.000	—	—
Ba	0.000	0.000	0.000	0.004	0.000	—	—	0.000	—
Total	0.024	0.018	0.016	1.891	0.000	—	—	1.992	0.000
Total cations	14.417	14.430	14.431	15.906	14.013	4.006	4.006	2.995	3.003
				Anions					
F	0.032	0.028	0.027	0.267	0.000	—	—	0.001	—
OH	0.968	0.972	0.973	3.733	—	—	—	—	—
$100Fe/(Fe + Mg)$	0.86	0.69	0.72	0.53	0.77	1.23	1.16	1.01	2.48

Note: Totals corrected for F = O. All Fe as FeO. b.d. = below detection. Dash = not determined. Be sought but not detected, that is, ≤0.002% BeO (in kornerupine). Also sought but not detected: Zn in spinel; Ni, Co in forsterite. Analyst of forsterite and spinel, M. Yates.
* Assumed ideal anion composition: 21 O + (OH,F) for kornerupine (Moore and Araki, 1979) and 20 O + 4(OH,F) for phlogopite.
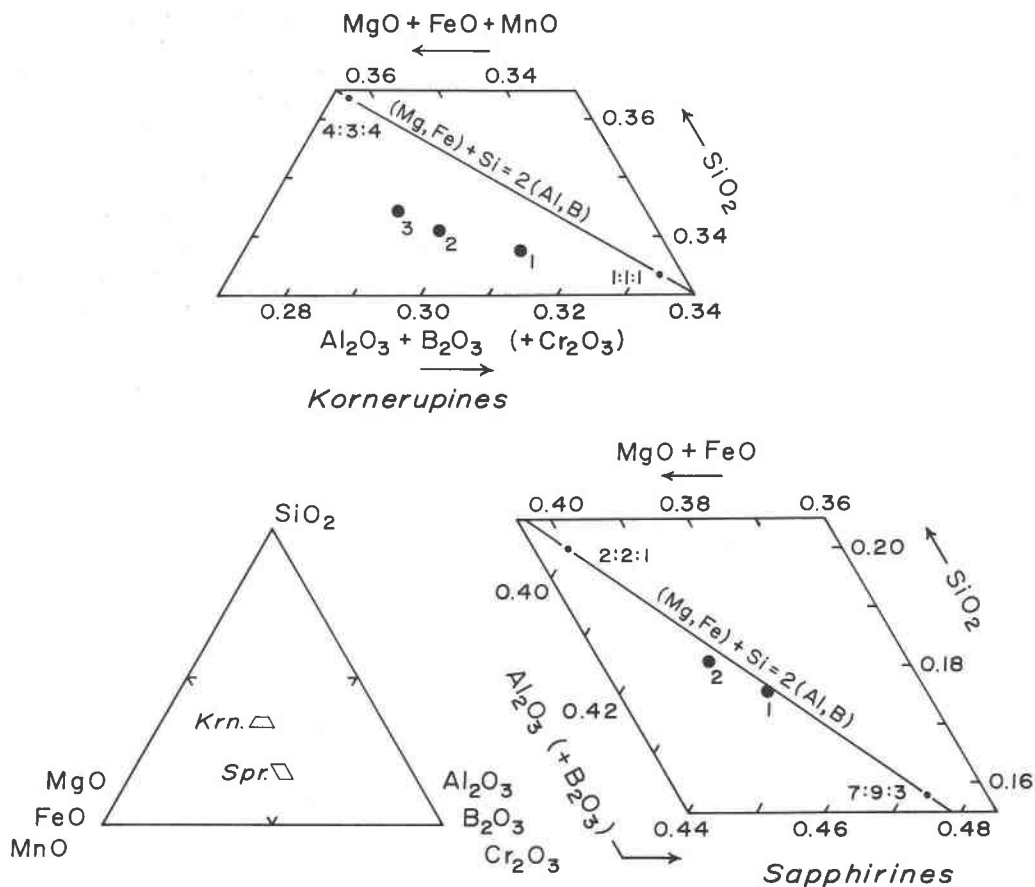
Fig. 6. Plot of kornerupine and sapphirine compositions in mole percent of SiO_2, $(FeO + MgO + MnO)$, and $(Al_2O_3 + B_2O_3)$. Numbers refer to analyses in Table 2 [except the composition of sapphirine 1, which is the average of two adjacent grains (Fig. 2) and is not listed].

Phlogopite, which changes little in composition from grain to grain, contains 26% of the hypothetical end member $NaMg_3(AlSi_3O_{10})(OH)_2$ (to be abbreviated in this paper as Naphl), but contains little Ti. The XII site is nearly fully occupied (95%). Phlogopites reported to contain a higher proportion of Naphl are found in schist with forsterite from Sar-e-Sang (X_{Na} = [Na/(Na + K)]$_{atomic}$ = 0.27 to 0.45, Kulke, 1976) and in association with Na-rich phlogopites in low-grade metaevaporites from Algeria (X_{Na} = 0.28, Schreyer et al., 1980). However, the Algerian phlogopite contains more Si (44.71% SiO_2) and less Al (11.16% Al_2O_3) than the Sar-e-Sang phlogopite in the kornerupine-bearing rock, which is closer in terms of SiO_2 and Al_2O_3 contents to the phlogopites (X_{Na} = 0.14 to 0.16; Grew et al., 1987) associated with kornerupine at Fiskenaesset, Greenland.

Magnesite, which appears also to be compositionally homogeneous, contains 45.00% MgO, 0.46% FeO, 0.48% CaO, and 0.08% MnO, corresponding to $Mg_{1.97}Fe_{0.01}$-$Ca_{0.02}(CO_3)_2$ with 100Fe/(Mg + Fe) = 0.56.

In contrast, kornerupine, sapphirine, and orthopyroxene vary in composition. Variations in sapphirine and orthopyroxene follow the Tschermak's substitution (Mg,

Fe) + Si ⇌ 2Al. Sapphirine compositions are intermediate between 7:9:3 and 2:2:1 in terms of $MgO:Al_2O_3:SiO_2$ (Fig. 6), in contrast to Schreyer and Abraham's (1975) peraluminous Sar-e-Sang sapphirines, which are considerably more aluminous than 7:9:3. Al_2O_3 contents of orthopyroxene vary from grain to grain (Table 2) and within a grain: three analyses on a third grain average 2.74% ± 0.12 Al_2O_3; a fourth analysis of this grain, 1.80% Al_2O_3. In the three kornerupines analyzed with the ion microprobe, compositional variations can be related by two substitutions: B ⇌ ^{IV}Al and Si + (Mg,Fe) ⇌ ^{IV}(B,Al) + ^{VI}Al. These substitutions appear to proceed concomitantly to the right such that (Al + B) decreases with increasing B (Fig. 7). The same substitutions were deduced for Fiskenaesset kornerupines, in which they were found to proceed independently of one another (Grew et al., 1987). Kornerupine compositions are intermediate between 1:1:1 and 4:3:4 and, in contrast to kornerupine from some other localities (e.g., Fiskenaesset, Grew et al., 1987), are less siliceous than the join between these two compositions (Fig. 6). This deviation from the idealized binary solution (ternary when B_2O_3 is considered; Werding and Schreyer, 1978) implies that kornerupine is in general a
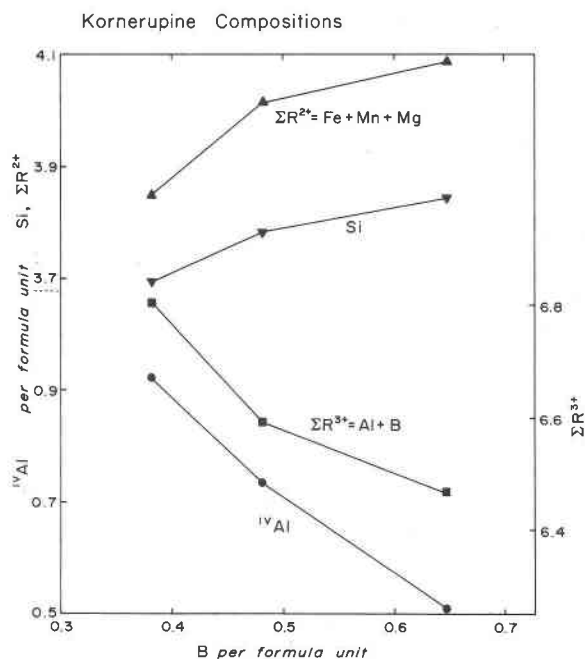
Kornerupine Compositions

Fig. 7. Variations of kornerupine $\Sigma R^{2+} = (Fe + Mn + Mg)$, Si, $\Sigma R^{3+} = (Al + B)$, and tetrahedral Al (= 5 − Si − B; Table 2) as a function of kornerupine B content.

TABLE 3. Mineral formulae and symbols (most are from Kretz, 1983)

Mineral	Symbol	Simplified formula
Albite	Ab	—
Andalusite	And	Al_2SiO_5
Chlorite	Chl	—
Cordierite	Crd	$Mg_2Al_4Si_5O_{18} \cdot 0.5H_2O$
Corundum	Crn	Al_2O_3
Enstatite	En	$MgSiO_3$
Forsterite	Fo	Mg_2SiO_4
Gedrite	Ged	$Na_{0.4}Mg_6Al_{2.4}Si_{6.6}O_{22}(OH)_2$
Kornerupine	Krn	$Mg_4Al_6B_{0.5}Si_4O_{21.5}(OH)$
Kyanite	Ky	Al_2SiO_5
Magnesite	Mgs	$MgCO_3$
Olivine	Ol	—
Orthopyroxene	Opx	—
Paragonite	Pg	—
Phlogopite*	Phl	$NaMg_3(AlSi_3)O_{10}(OH)_2$
Quartz	Qtz	SiO_2
Sapphirine	Spr	$Mg_7Al_{18}Si_3O_{40}$
Spinel	Spl	$MgAl_2O_4$
Sillimanite	Sil	Al_2SiO_5
Talc	Tlc	$Mg_3Si_4O_{10}(OH)_2$
Tourmaline	Tur	$NaMg_3Al_6Si_6B_3O_{27}(OH)_4$

* Hypothetical pure-Na end member.

quaternary solid solution in the system $MgO-Al_2O_3-SiO_2-B_2O_3$. Li content of kornerupine is variable, whereas its F content is relatively constant.

About 0.034 wt% B_2O_3 was found in the forsterite, which is equivalent to 0.1 mol% sinhalite ($MgAlBO_4$) in solid solution.

Compositional relationships and attainment of equilibrium

Variations in sapphirine Al content may be related to variations in Al content of contiguous kornerupine, that is, the contiguous pair kornerupine 1–sapphirine 1 is more aluminous than the contiguous pair kornerupine 2–sapphirine 2 (Table 2, Fig. 6). Thus, sapphirine Al_2O_3, SiO_2, and MgO contents appear to be controlled by the Al_2O_3 and B_2O_3 contents of associated kornerupine. On the other hand, the variations in Al contents of orthopyroxene appear not to be related to kornerupine Al_2O_3 contents and may be due instead to the effects of later metamorphic events, as similar variation has been reported from other terranes (e.g., Enderby Land, Antarctica, Ellis et al., 1980).

The fluorine K_D [= $(F/OH)_{Phl}/(F/OH)_{Krn}$], assuming ideal anion compositions, ranges from 2.2 to 2.6, values in the upper range for coexisting kornerupine and phlogopite-biotite from other areas (Grew et al., 1985, and unpub. data). Kornerupine is enriched not only in B but also in Li relative to phlogopite and sapphirine, a feature characteristic of other kornerupine-bearing rocks (Grew, 1986; Grew et al., 1985, 1987).

The minerals increase in $100X_{Fe}$ as follows: phlogopite

(0.53) < magnesite (0.56) < kornerupine (0.60–0.86) ≈ sapphirine (0.70–0.77) < forsterite (1.01) < orthopyroxene (1.18–1.28) < spinel (2.48). The sequence phlogopite < kornerupine < orthopyroxene < spinel in the Sar-e-Sang rock is similar to kornerupine-bearing rocks from other localities (e.g., Waters and Moore, 1985; Grew et al., 1987). The fractionation of Fe and Mg between magnesite and orthopyroxene is close to that reported by Evans and Trommsdorff (1974), that is, K_D = $(Fe/Mg)_{En}/(Fe/Mg)_{Mgs}$ = 2.0–2.3 (for mineral abbreviations, see Table 3) in the Sar-e-Sang rock compared to 1.0–2.0 in the Alpine rocks analyzed by Evans and Trommsdorff (1974).

The Fe-Mg fractionation between kornerupine and sapphirine varies in the Sar-e-Sang rock. The sequence for two contiguous pairs is kornerupine 1 ($100X_{Fe} = 0.86$) > sapphirine 1 (0.70) and sapphirine 2 (0.77) > kornerupine 2 (0.69). As the kornerupine in the first pair contains less B_2O_3 than that in the second pair (1.83% vs. 2.28%), the reversal may be due to the effect of B on Fe-Mg fractionation. Grew et al. (1987) suggested that kornerupine becomes more magnesian relative to associated minerals as its B content increases. However, at the low concentrations of Fe found in the Sar-e-Sang minerals, analytical errors and small amounts of Fe^{3+} could also explain the reversal in Fe-Mg fractionation between kornerupine and sapphirine.

The sequence $X_{Mg}^{Ol} > X_{Mg}^{Opx}$ in the Sar-e-Sang rock is not commonly found elsewhere; other examples are a sapphirine-bearing rock from the Fiskenaesset area, Greenland ($X_{Fe}^{Ol} = 0.04 < X_{Fe}^{Opx} = 0.05$ (Williams, 1984), and a magnesian skarn from the southwest Pamirs, USSR ($X_{Fe}^{Ol} = 0.026 < X_{Fe}^{Opx} = 0.032$; Zotov, 1968). This sequence is not predicted by ideal solid-solution models in which the more common $X_{Fe}^{Ol} > X_{Fe}^{Opx}$ is assumed (e.g., Medaris, 1969). However, if nonideal solid solution is postulated for either olivine or orthopyroxene, a reversal
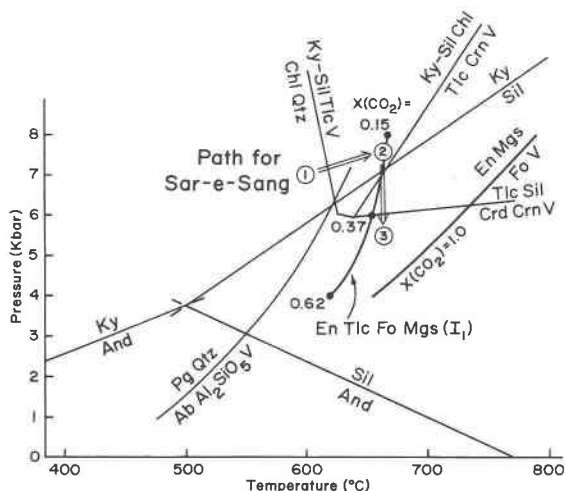
Fig. 8. Pressure-temperature diagram for metamorphism at Sar-e-Sang (arrows). Sources of data are as follows: Al_2SiO_5—Holdaway (1971); Pg + Qtz breakdown—Chatterjee (1972); reactions among Chl, Qtz, Ky, Tlc, Sil, Crn, and Crd—Massonne and Schreyer (1983) and Grew and Sandiford (1984); and En + Mgs + Fo ± Tlc equilibria and X_{CO_2} = CO_2/(CO_2 + H_2O) molar values—R. Berman (pers. comm., 1987) calculated from data of Chernosky and Berman (1986 and in prep.). Circled numbers refer to the metamorphic stages of Schreyer and Abraham (1976). Metastable extensions for reactions in the MgO-Al_2O_3-SiO_2-H_2O system have been deleted, as have kinks in the reaction curves at the Ky = Sil curve. Mineral abbreviations are given in Table 3. The univariant equilibrium assemblage En + Tlc + Fo + Mgs corresponds to the invariant point I_1 in the μ_{H_2O}-μ_{CO_2} diagram (Fig. 9).

of the usual X_{Fe}^{Ol} > X_{Fe}^{Opx} is predicted in magnesian pairs. Sack (1980) calculated that olivine is more magnesian than orthopyroxene at temperatures between 500 and 800 °C and at olivine X_{Fe} values below 0.1–0.25 (depending on the temperature).

In summary, the observed sequence of X_{Fe} values in the Sar-e-Sang rock is probably an equilibrium one because it is similar to that found in comparable rocks elsewhere. Moreover, Al distribution between kornerupine and sapphirine is regular, a feature consistent with equilibrium (Zen, 1963). On the other hand, compositional variations from grain to grain in kornerupine, sapphirine, and enstatite would not be expected if the minerals had equilibrated with one another over the entire volume of the rock. Possibly, the variations in kornerupine B contents are relics of heterogeneous distribution of B in the original sedimentary rock that were not eliminated by redistribution during metamorphism. I suggested above that the precursor to the kornerupine rock may be an argillaceous sedimentary rock. In a review of B contents of argillaceous sediments, Harder (1959) showed that the B tended to be concentrated in the finer-grained fractions, those rich in illite and chlorite. Thus, B_2O_3 contents could have varied over short (<1 mm) distances in an otherwise homogeneous sediment. During recrystallization of

the clay minerals into kornerupine, redistribution of B may not have been complete. Heterogeneous distribution of SiO_2 in the original sediment may explain the appearance of enstatite and sapphirine in one patch of the present rock and spinel in another. Consequently, the minerals must have equilibrated with one another only over very small (<1 mm³) volumes of rock, a situation analogous to the "mosaic equilibrium" Korzhinskiy (1957, 1973) proposed for rocks undergoing metasomatism (see also Zen, 1963).

PHYSICAL CONDITIONS OF METAMORPHISM

Schreyer and Abraham (1976) deduced a three-stage metamorphic evolution for the Sar-e-Sang whiteschist as follows: (1) Chl + Qtz + Ky, Chl + Qtz + Tlc, Pg, Pg + Qtz(?); (2) Tlc + Ky ± Ged; (3) Tlc + Crd + Crn, Sil. Schreyer and Abraham further suggested that this succession of assemblages resulted largely from decreases in water activity in the fluid phase, whereas changes in pressure and temperature were comparatively modest. Their estimate for the third stage was 5–6 kbar and 640 °C. More recent experimental data confirm these pressure-temperature estimates. The results of Massonne et al. (1981) and Massonne and Schreyer (1983) on talc-Al_2SiO_5 stability, in conjunction with theoretical and other experimental data, suggest a modest overall decrease in pressure and increase in temperature: ≥6 kbar, ≤600 °C for the first stage, ≥7 kbar, 630–670 °C for the second stage, and ≤6 kbar, 650–670 °C for the third stage of metamorphism at Sar-e-Sang (Fig. 8). The temperature increase would be less if P_{H_2O} decreased more than lithostatic pressure, as Schreyer and Abraham (1976) proposed.

The magnesite + enstatite assemblage can provide some constraints on the composition of the fluid phase that equilibrated with the kornerupine-bearing rock. Because only a small amount of Al_2O_3 and FeO are present in these minerals, direct application of theoretical and experimental data for the MgO-SiO_2-H_2O-CO_2 system (e.g., Greenwood, 1967; Johannes, 1969; Schreyer et al., 1972; Ohnmacht, 1974) is possible. On the basis of the most current set of available thermodynamic data (Berman et al., 1985; Chernosky and Berman, 1986 and in prep.), R. Berman (pers. comm., 1987) calculated T-X_{CO_2} phase diagrams [where X_{CO_2} = CO_2/(CO_2 + H_2O) in the fluid phase] for assemblages involving magnesite, talc, anthophyllite, enstatite, and forsterite. Some curves resulting from Berman's calculations are presented in Figure 8.

Magnesite-enstatite is stable at X_{CO_2} ≥ 0.25 (7 kbar) and ≥0.15 (8 kbar), the X_{CO_2} values for the univariant assemblage En + Mgs + Fo + Tlc at temperatures near 660 °C. Talc and forsterite do not appear to have equilibrated with Mgs + En in the kornerupine-bearing rock, and thus these X_{CO_2} values are minima. On the other hand, X_{CO_2} values may not have greatly exceeded the minimum values, because the kornerupine-bearing rock probably equilibrated with relatively hydrous fluids associated with the whiteschists, as discussed in the next section.

A final consideration is whether the kornerupine-bearing rock crystallized during Schreyer and Abraham's (1976) second or the third stage of metamorphism. There is little textural evidence in the kornerupine-bearing rock for a multistage history; the tendency for kornerupine to enclose sapphirine and isolate forsterite is not conclusive. However, the presence of a well-defined schistosity in the kornerupine-bearing rock, a texture indicative of recrystallization during deformation, suggests that the present assemblage in that rock developed during the second stage. Schreyer and Abraham (1976) concluded that the second stage took place under deformation, which resulted in the schistosity of the whiteschist. In contrast, they attribute the third stage to a period of static metamorphism. The third stage apparently had little effect on the mineral assemblage in the kornerupine-bearing rock, although it may have caused some of the variations in the Al_2O_3 content of enstatite (see above).

In summary, the whiteschists and the kornerupine-bearing rock are presumed to have crystallized during the second stage under the same pressure-temperature conditions, most likely 7–8 kbar, 630–670 °C. These rocks are inferred to have been collected sufficiently close to one another so that spatial variations in pressure and temperature were probably negligible. However, gradients in fluid composition between the two rocks may have been substantial. The kornerupine-bearing rock crystallized under conditions of higher CO_2. The assemblage enstatite + magnesite is stable at X_{CO_2} values of the univariant En + Mgs + Tlc + Fo assemblage or somewhat higher, that is, $X_{CO_2} \geq 0.15$ at 7–8 kbar (Fig. 8).
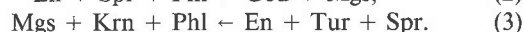
PHASE RELATIONS AT SAR-E-SANG

The purpose of the present section is to construct a diagram by the Schreinemakers method relating the distribution of kornerupine and tourmaline to variations in the chemical potentials (μ) of CO_2 and H_2O at constant pressure and temperature, an approach developed by Korzhinskiy (1957, 1973). The critical phases in the kornerupine-bearing rock and in the whiteschist can be approximated by the model system $MgO-Al_2O_3-SiO_2-B_2O_3$-$Na_2O-CO_2-H_2O$. These phases are kornerupine, magnesite, phlogopite, enstatite, sapphirine, talc, tourmaline, gedrite, and kyanite (sillimanite). For construction of a μ_{H_2O}-μ_{CO_2} diagram, I will not be considering the phases of this model system stable only during the first stage (chlorite, paragonite) or the third stage (cordierite, corundum, plagioclase) or phases of sporadic occurrence (quartz). These restrictions on the number of phases are necessary for the construction of a μ_{H_2O}-μ_{CO_2} diagram to be manageable.

The amounts of FeO in these rocks are probably too small to affect phase relations to a significant extent. K_2O is a significant component only of phlogopite. In my treatment of the phase relations, Naphl is included as one of the phases. The deduced assemblages containing Naphl are undoubtedly metastable relative to assemblages lacking Naphl. However, in the presence of K_2O, the assem-
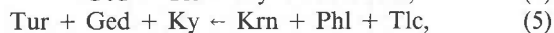
blages with phlogopite are interpreted to be stable. Formation of Naphl in the model system means Na enrichment of phlogopite in the K_2O-bearing system. Breakdown of Naphl means K enrichment of phlogopite. In this way, Na_2O can be treated as an inert component, and reactions involving tourmaline, kornerupine, and gedrite can be balanced. B_2O_3 will also be considered as an inert component. The marked variations in kornerupine B content (Table 2) are evidence against control of B activities by an external reservoir. CO_2 and H_2O will be treated as fully mobile components. With these assumptions, I will attempt to relate the kornerupine and tourmaline assemblages (all with Naphl) in terms of a μ_{CO_2}-μ_{H_2O} diagram at constant temperature and pressure (Fig. 9). Mineral formulae used in constructing the diagram (Table 3) are either simplified from the measured compositions (Table 2; Schreyer and Abraham, 1976) or are ideal compositions. The B content of the kornerupine was estimated from the whole-rock B_2O_3 content (0.55 wt%) and the modal amount of kornerupine. Many reactions in Figure 9 appear to be little affected by the B content assumed for kornerupine in the range B = 0.3 to 0.5 per formula unit.

Figure 9 is only a portion of one of the possible μ_{CO_2}-μ_{H_2O} diagrams involving the phases Ky, Tur, En, Tlc, Phl, Ged, Krn, Spr, Mgs, Spl, and Fo. The test recommended by Burt (1978) to justify the choice of metastable and stable invariant points has not been attempted. In this diagram, the Krn-Mgs-Phl-En-Spr assemblage has a limited stability range. It is bounded by three reactions (left side observed in the assemblage; numbering same as in Fig. 9):

$$Spr + En \leftarrow Ky + Mgs, \qquad (1)$$
$$En + Spr + Phl \leftarrow Ged + Mgs, \qquad (2)$$
$$Mgs + Krn + Phl \leftarrow En + Tur + Spr. \qquad (3)$$

In Reactions 2 and 3, Naphl is also a product, thereby implying that the associated phlogopite should be enriched in Naphl. The phlogopite in the kornerupine-bearing rock contains 26% of Naphl, twice the proportion reported by Schreyer and Abraham (1976) in a phlogopite included in gedrite and more than most other metamorphic phlogopites and biotites (e.g., Guidotti, 1984).

In contrast, the Tur + Tlc + Ky ± Ged assemblage in the whiteschist has a more extended stability range bounded by three reactions:

$$Ged + Tlc \leftarrow Ky + En + Phl, \qquad (4)$$
$$Tur + Ged + Ky \leftarrow Krn + Phl + Tlc, \qquad (5)$$
$$Ged \leftarrow Mgs + Phl + Tlc + Ky. \qquad (6)$$

This stability field overlaps that for the kornerupine assemblage, particularly as the relative μ_{H_2O} values for the invariant points [Ky, Tlc] and [En, Spr] cannot be unambiguously determined (one of three alternatives is shown in Fig. 9). However, Schreyer and Abraham's (1975, 1976) report of tourmaline and "metastable" sapphirine in cordierite reaction rims between kyanite and gedrite in sample SSg42a (see above) suggests that this
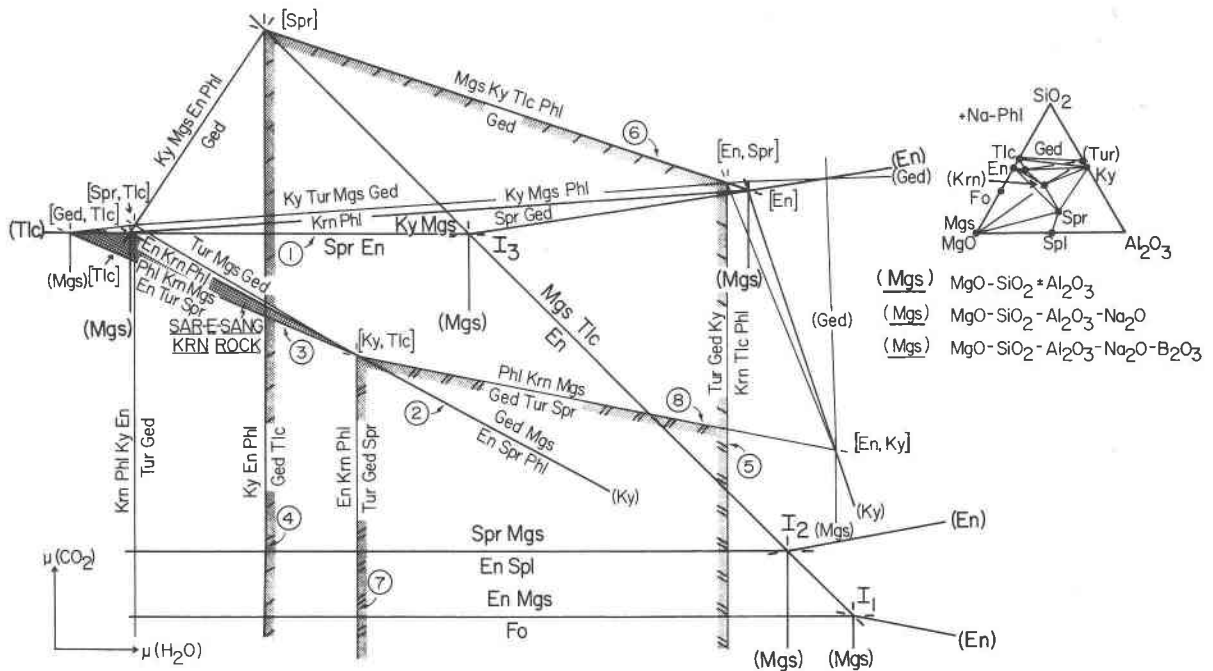
Fig. 9. μ_{CO_2}-μ_{H_2O} diagram constructed by the Schreinemakers method. Univariant reactions are indicated either by the phases involved or by the one phase (in rounded brackets) not involved; invariant points are indicated by the phases (in square brackets) not involved (convention of Burt, 1978). Mineral abbreviations are from Table 3; B-bearing phases are enclosed in rounded brackets in the compositional plot. The four systems (two are combined) included in the diagram are shown by different letter sizes and line thicknesses, as summarized in the legend. The numbered reactions are discussed in the text. Light shading indicates the range of stability for the assemblage Krn + Phl + Mgs + En + Spr, single hachures and shading indicate the field of stability for the whiteschist assemblage Tur + Ged + Tlc + Ky, and double hachures and shading, that for the assemblage Ged + Tur + Spr + Ky.

rock may have recrystallized during the third stage at μ_{CO_2}-μ_{H_2O} conditions corresponding to the stability field of the Spr + Tur + Ged assemblage. The Spr + Tur + Ged assemblage is incompatible with both Krn + En and Krn + Mgs because of the reactions (Fig. 9):

$$\text{Tur} + \text{Ged} + \text{Spr} \leftarrow \text{Krn} + \text{En} + \text{Phl} \quad (7)$$
$$\text{Tur} + \text{Ged} + \text{Spr} \leftarrow \text{Krn} + \text{Mgs} + \text{Phl} \quad (8)$$

and thus forms at higher μ_{H_2O} and lower μ_{CO_2} than the assemblage Krn + Mgs + En + Phl of the kornerupine-bearing rock. Because water activity probably decreased during the transition from the second to the third stage (Schreyer and Abraham, 1976), the second-stage whiteschist assemblage must have also formed at higher μ_{H_2O} and lower μ_{CO_2} than the kornerupine-bearing assemblage. Thus the intuitively reasonable conclusion that the whiteschist formed under higher water activities than the kornerupine rock can be justified in terms of the μ_{H_2O}-μ_{CO_2} relations illustrated in Figure 9.

DISTRIBUTIONS OF TOURMALINE AND KORNERUPINE

The main compositional difference between kornerupine and tourmaline is that kornerupine contains less Na_2O, SiO_2, B_2O_3 and H_2O. Consequently, at a given pressure and temperature, the distribution of these two minerals will be controlled by the availability of these components. The whole-rock analyses of the Sar-e-Sang rocks (Table 1 and Schreyer and Abraham, 1976) imply that the availability of Na_2O and B_2O_3 could not have affected the distribution of kornerupine and tourmaline, because the kornerupine-bearing rock contains more Na_2O and B_2O_3 than the tourmaline-bearing whiteschist. The main difference between the rocks is their SiO_2 (Fig. 5) and CO_2 contents. The difference in SiO_2 [after projection through (K,Na)-phlogopite] is so great that the only mineral common to both rocks is phlogopite and there are no crossing tie lines (except for the possible gedrite-sapphirine join). Consequently, SiO_2 appears to be the main control on the mineral content of the two rocks, whereas H_2O and CO_2 activities are of secondary importance.

The role of SiO_2 is more obvious if we consider the possibility of whiteschist with kornerupine and the converse, a magnesite-bearing rock with tourmaline. The appearance of kornerupine with talc involves a hydration (see Reaction 5, Fig. 9; mineral compositions from Table 3):

$$6\text{Krn} + 6.3\text{Phl} + 13.2\text{Tlc} \rightleftharpoons \text{Tur} + 13.25\text{Ged} + 2.25\text{Ky} + 7.25\text{H}_2\text{O}.$$
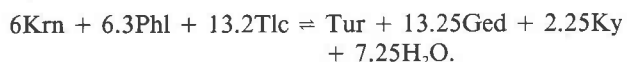
Thus Krn + Tlc requires a higher μ_{H_2O} than Tur + Ged +

Ky + Tlc. These high water activities appear to be rarely, if ever, attained in nature. Although Tur + Tlc ± Qtz is not unusual (e.g., Vrána and Barr, 1972; Grew and Sandiford, 1984) Krn + Tlc is rare, and the two reported instances (McKie, 1965; Vrána and Barr, 1972) have not been definitively documented as equilibrium assemblages. Moreover, in the tourmaline-bearing cordierite reaction rim between gedrite and kyanite described by Schreyer and Abraham (1976), a possible reaction for kornerupine formation would be a hydration:

$$6Krn + 5.4Phl + 14.1Crd \rightleftharpoons Tur + 10.9Ged + 32.9Ky + 2.55H_2O. \qquad (9)$$
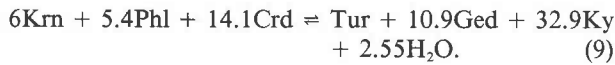
Consequently, the appearance of kornerupine during the third stage in the whiteschist (even in a silica-undersaturated patch) is also unlikely.

Conversely, the appearance of tourmaline in the magnesite rock is theoretically possible only with a marked increase in this rock's overall B content. For tourmaline to appear in Ged + Ky + Mgs or similar assemblages in bulk compositions equivalent to the kornerupine-bearing rock, that is, under conditions where Krn + Phl is not stable, μ_{CO_2} must be greater than that indicated for the present kornerupine-bearing assemblage (Fig. 9). Such high μ_{CO_2} values appear not to have been attained with the mixed H_2O-CO_2 fluids present during metamorphism at Sar-e-Sang or at other whiteschist localities.

A final point concerns possible changes in the bulk compositions of the Sar-e-Sang rocks during metamorphism. Except for minor loss of volatiles, such changes were probably very small. In particular, the precursor to the kornerupine-bearing rock probably contained magnesite and was not "carbonated" during metamorphism. If MgO had not been fixed in magnesite, this bulk composition (minus CO_2) would have recrystallized at low μ_{H_2O} to Fo + En + Spl + Krn. For tourmaline to appear in this assemblage with no change in bulk B content requires a dehydration,

$$6Krn + Phl + 12.5Fo \rightleftharpoons Tur + 33.5En + 15.5Spl + 2H_2O, \qquad (10)$$
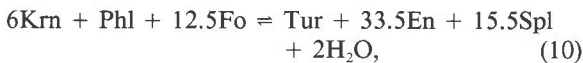
and thus the Krn + Fo assemblage, like the Krn + Mgs assemblage, would have formed under less extreme conditions than the equivalent tourmaline-bearing assemblage.

In summary, a kornerupine-bearing whiteschist and a tourmaline + magnesite (or tourmaline + forsterite) rock (for rocks with <1% B_2O_3) require fluids extremely rich in H_2O and CO_2 (or poor in H_2O), respectively, which are unlikely to occur under geologic conditions. The observed assemblages are possibly the most stable ones that can equilibrate with a mixed CO_2-H_2O fluid given the starting compositions of the sedimentary precursors. The compositions of the fluids associated with Krn + Mgs (or Krn + Fo) and Tur + Tlc are closer to one another in CO_2/H_2O ratio than the extreme compositions associated with Krn + Tlc and Tur + Mgs (or Tur + Fo), thereby minimizing μ_{CO_2} and μ_{H_2O} gradients between layers. During metamorphism of the Sar-e-Sang whiteschist-marble sequence, the tendency for μ_{CO_2} and μ_{H_2O} to be equalized over all layers by some outside reservoir (the assumption that CO_2 and H_2O are perfectly mobile components) is counteracted by the buffering capacity of the mineral assemblages. The large difference in SiO_2 contents (and to a lesser extent, CO_2 contents) between the whiteschist and kornerupine-bearing rock was sufficient to maintain μ_{CO_2} gradients between the two rocks. From this perspective, the difference in SiO_2 content was the main factor in controlling tourmaline and kornerupine distribution at Sar-e-Sang, whereas differences in μ_{CO_2} and μ_{H_2O} of the metamorphic fluid phase played a subordinate role.

CONCLUSIONS

The results of this study suggest that many kornerupine-forming reactions are hydrations. Yet kornerupine contains less water than tourmaline and, unlike tourmaline, is largely found in high-grade rocks. The keys to this paradox are that the Na released from tourmaline breakdown is assumed to be taken up by phlogopite and that the B/OH ratio assumed for kornerupine (0.5 B per formula unit and B/OH = 0.5) is lower than that assumed for tourmaline (B/OH = 0.75). As a result, the Krn + Phl combination is more hydrous than Tur for a given content of B.

That kornerupine formation could be a hydration was a conclusion also reached in my study with R. K. Herd and N. Marquez (Grew et al., 1987) on kornerupine-forming reactions involving sodian phlogopite ($X_{Na} = 0.14$–0.16) but not tourmaline in the highly magnesian granulite-facies rocks of the Fiskenaesset complex (Greenland).

However, the reactions proposed for Sar-e-Sang and Fiskenaesset are applicable only to magnesian, silica-undersaturated rocks. In rocks of this composition, kornerupine appears to be more common than tourmaline in granulite-facies terranes. In the far more abundant and geologically important rocks of pelitic composition, tourmaline and kornerupine are rare in the granulite facies, whereas tourmaline is virtually ubiquitous in the amphibolite facies (e.g., Grew, 1986). The question concerning the distribution of tourmaline and kornerupine in metapelites is thus pertinent to understanding the transition between the amphibolite and granulite facies, especially changes in the composition of the metamorphic fluid phase. However, a resolution to this question requires a different approach than that presented here for the highly magnesian, silica-undersaturated rocks.

Metapelites are richer in Fe (Fe/Mg ratio is higher) and silica than the magnesian rocks from Sar-e-Sang and Fiskenaesset. As a result, most of the Na is accommodated in plagioclase, and tourmaline-breakdown reactions involve albite instead of Na-rich phlogopite. Kornerupine in metapelites contains more B and Fe than the Sar-e-Sang and Fiskenaesset kornerupines and is commonly stable with quartz (e.g., Girault, 1952; Grew and Hinthorne, 1983). Thus the role played by SiO_2 content is

much reduced. One possible breakdown reaction for tourmaline in metapelites is:

$$Sil + Tur + Garnet \rightleftharpoons Krn + Qtz + Plagioclase$$
$$\pm H_2O. \qquad (11)$$
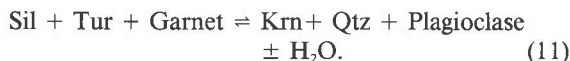
Reaction 11 involves little, if any, loss of water unless B_2O_3 is also lost (Grew, 1987).

In contrast to the situations at Sar-e-Sang and Fiskenaesset, a reaction such as 11 may involve an anatectic melt. In this case, H_2O and B_2O_3 may be incorporated in the melt, and the resulting kornerupine-bearing assemblage ("restite") can be regarded as dehydrated relative to its tourmaline-bearing precursor. If all the B_2O_3 were incorporated in the melt, kornerupine could not form, and thus anatexis is a possible cause of B depletion in granulite-facies metapelites. However, Manning and Pichavant (1983) have suggested that B_2O_3 may not be extensively incorporated in anatectic melts, but either remains in the restites or is dissolved in late pneumatolytic fluids. In the latter case, the system would become open to B, and B could be lost from the rock unless fluid compositions were buffered by some mechanism, such as a kornerupine + tourmaline + biotite ± melt assemblage (Grew, 1986). In summary, the behavior of B during high-grade metamorphism of pelitic rocks, in which B is generally believed to be relatively mobile, involves several chemical and physical variables, none of which are well understood at present. As emphasized by Manning and Pichavant (1983), more experimental and mineralogical studies are needed to understand the role of B in high-grade metamorphic processes. Such studies could also add a new perspective on the closely related questions of the role of C-H-O fluids in granulite-facies metamorphism and the nature of the amphibolite- to granulite-facies transition.

REFERENCES CITED

Berman, R.G., Greenwood, H.J., and Brown, T.H. (1985) An internally consistent thermodynamic data base for minerals in the system $Na_2O-K_2O-MgO-CaO-FeO-Al_2O_3-SiO_2-TiO_2-CO_2$. Atomic Energy of Canada TR-377.

Blaise, J., and Cesbron, Fabien. (1966) Données minéralogiques et pétrographiques sur le gisement de lapis-lazuli de Sar-e-Sang, Hindou-Kouch, Afghanistan. Bulletin de la Société française de Minéralogie et Cristallographie, 89, 333–343.

Burt, D.M. (1978) Multisystems analysis of beryllium mineral stabilities: The system $BeO-Al_2O_3-SiO_2-H_2O$. American Mineralogist, 63, 664–676.

Chatterjee, N.D. (1972) The upper stability limit of the assemblage paragonite + quartz and its natural occurrences. Contributions to Mineralogy and Petrology, 34, 288–303.

Chernosky, J.V., and Berman, R.G. (1986) Experimental reversal of the equilibrium: clinochlore + 2 magnesite = 3 forsterite + spinel + 2 CO_2 + 4 H_2O (abs.). EOS, 67, 1279.

Ellis, D.J., Sheraton, J.W., England, R.N., and Dallwitz, W.B. (1980) Osumilite-sapphirine-quartz granulites from Enderby Land, Antarctica—Mineral assemblages and reactions. Contributions to Mineralogy and Petrology, 72, 123–143.

Evans, B.W., and Trommsdorff, Volkmar. (1974) Stability of enstatite + talc, and CO_2-metasomatism of metaperidotite, Val d'Efra, Lepontine Alps. American Journal of Science, 274, 274–296.

Girault, J.P. (1952) Kornerupine from Lac Ste. Marie, Quebec, Canada. American Mineralogist, 37, 531–541.

Greenwood, M.J. (1967) Mineral equilibria in the system $MgO-SiO_2-H_2O-CO_2$. In P.H. Abelson, Ed., Researches in geochemistry, p. 542–567. Wiley, New York.

Grew, E.S. (1986) Petrogenesis of kornerupine at Waldheim (Sachsen), German Democratic Republic. Zeitschrift für Geologische Wissenschaften, 14, 525–558.

——— (1987) A second occurrence of kornerupine in Waldheim, Saxony, German Democratic Republic. Zeitschrift für geologische Wissenschaften, in press.

Grew, E.S., and Hinthorne, J.R. (1983) Boron in sillimanite. Science, 221, 547–549.

Grew, E.S., and Sandiford, M. (1984) A staurolite-talc assemblage in tourmaline-phlogopite-chlorite schist from northern Victoria Land, Antarctica, and its petrogenetic significance. Contributions to Mineralogy and Petrology, 87, 337–350.

Grew, E.S., Hinthorne, J., Marquez, N., Werding, G., and Abraham, K. (1985) Li, Be, B, and F in kornerupine petrogenesis (abs.). EOS, 66, 1147.

Grew, E.S., Hinthorne, J.R., and Marquez, N. (1986) Li, Be, B, and Sr in margarite and paragonite from Antarctica. American Mineralogist, 71, 1129–1134.

Grew, E.S., Herd, R.K., and Marquez, N. (1987) Boron-bearing kornerupine from Fiskenaesset, West Greenland: A re-examination of specimens from the type locality. Mineralogical Magazine, 51, 695–708.

Grew, E.S., Belakovskiy, D.I., and Leskova, N.V. (1988) Fazovyye ravnovesiya talk-kianit-rogovoobmankovykh porodakh (s andaluzitom i sillimanitom) iz Kugi-Lalya, yugo-zapadnyy Pamir [Phase equilibria in talc-kyanite-hornblende rocks (with andalusite and sillimanite) from Kugi-Lal, southwestern Pamirs]. Doklady Akademii Nauk SSSR, in press.

Guidotti, C.V. (1984) Micas in metamorphic rocks. Mineralogical Society of America Reviews in Mineralogy, 13, 357–467.

Harder, Hermann. (1959) Beitrag zur Geochemie des Bors. Teil II, Bor in Sedimenten. Nachrichten der Akademie der Wissenschaften in Göttingen. Mathematisch-Physikalische Klasse, Jahrgang 1959, 123–183.

Henry, D.J., and Guidotti, C.V. (1985) Tourmaline as a petrogenetic indicator mineral: An example from the staurolite-grade metapelites of NW Maine. American Mineralogist, 70, 1–15.

Holdaway, M.J. (1971) Stability of andalusite and the aluminum silicate phase diagram. American Journal of Science, 271, 97–131.

Johannes, W. (1969) An experimental investigation of the system $MgO-SiO_2-H_2O-CO_2$. American Journal of Science, 267, 1083–1104.

Korzhinskiy, D.S. (1947) Bimetasomaticheskiye flogopitovyye i lazuritovyye mestorozhdeniya arkheya Pribaykalya (Bimetasomatic phlogopite and lapis lazuli deposits of the Archean of Pribaikalya). Trudy Instituta geologicheskikh nauk Akademii nauk SSSR, vypusk 29.

——— (1957) Fiziko-Khimicheskiye Osnovy Analiza Paragenezisov Mineralov. USSR Academy of Sciences, Moscow (English translation: Physico-chemical basis of the analysis of the paragenesis of minerals. Consultants Bureau, New York, 1959).

——— (1973) Teoreticheskiye Osnovy Analiza Paragenezisov Mineralov (Theoretical Basis for the Analysis of Mineral Parageneses). Nauka, Moscow.

Kretz, Ralph. (1983) Symbols for rock-forming minerals. American Mineralogist, 68, 277–279.

Kulke, H.H.G. (1976) Metamorphism of evaporitic carbonate rocks (NW

Africa and Afghanistan) and the formation of lapis lazuli. 25th International Geological Congress, Sydney, Abstracts, 1, 131–132.

Kulke, H.H.G., and Schreyer, Werner. (1973) Kyanite-talc schist from SareSang, Afghanistan. Earth and Planetary Science Letters, 18, 324–328.

Manning, D.A.C., and Pichavant, Michel. (1983) The role of fluorine and boron in the generation of granitic melts. In M.P. Atherton and C.D. Gribble, Eds., Migmatites, melting and metamorphism, p. 94–109. Shiva, Cheshire, England.

Massonne, H.-J., and Schreyer, Werner. (1983) Stability of the talc-kyanite assemblage revisted (abs.). Terra Cognita, 3, 187.

Massonne, H.-J., Mirwald, P.W., and Schreyer, Werner. (1981) Experimentelle Überprüfung der Reaktionskurve Chlorit + Quarz = Talk + Disthen im System $MgO-Al_2O_3-SiO_2-H_2O$. Fortschritte der Mineralogie, 59, 122–123.

McKie, D. (1965) The magnesium aluminum borosilicates: Kornerupine and grandidierite. Mineralogical Magazine, 34, 346–357.

Medaris, L.G., Jr. (1969) Partitioning of Fe^{++} and Mg^{++} between coexisting synthetic olivine and orthopyroxene. American Journal of Science, 267, 945–968.

Moine, B., Sauvan, P., and Jarousse, J. (1981) Geochemistry of evaporite-bearing series: A tentative guide for the identification of metaevaporites. Contributions to Mineralogy and Petrology, 76, 401–412.

Moore, P.B., and Araki, Takaharu. (1979) Kornerupine: A detailed crystal-chemical study. Neues Jahrbuch für Mineralogie Abhandlungen, 134, 317–336.

Ohnmacht, W. (1974) Petrogenesis of carbonate-orthopyroxenites (sagvandites) and related rocks from Troms, northern Norway. Journal of Petrology, 15, 303–323.

Pichavant, Michel, and Manning, D.A.C. (1984) Petrogenesis of tourmaline granites and topaz granites; the contribution of experimental data. Physics of the Earth and Planetary Interiors, 35, 31–50.

Plimer, I.R. (1983) The association of tourmaline-bearing rocks with mineralisation at Broken Hill, N.S.W. Australian Institute of Mining and Metallurgy Conference, Broken Hill, N.S.W., 1983, Proceedings, p. 157–176.

Robbins, C.R., and Yoder, H.S., Jr. (1962) Stability relations of dravite, a tourmaline. Carnegie Institution of Washington Year Book, 61, 106–108.

Sack, R.O. (1980) Some constraints on the thermodynamic mixing properties of Fe-Mg orthopyroxenes and olivines. Contributions to Mineralogy and Petrology, 71, 257–269.

Schreyer, W. (1973) Whiteschist: A high-pressure rock and its geologic significance. Journal of Geology, 81, 735–739.

Schreyer, Werner, and Abraham, Kurt. (1975) Peraluminous sapphirine as a metastable reaction product in kyanite-gedrite-talc schist from Sar e Sang, Afghanistan. Mineralogical Magazine, 40, 171–180.

——— (1976) Three-stage metamorphic history of a whiteschist from Sar e Sang, Afghanistan, as part of a former evaporite deposit. Contributions to Mineralogy and Petrology, 59, 111–130.

Schreyer, Werner, Ohnmacht, W., and Mannchen, J. (1972) Carbonate-orthopyroxenites (sagvandites) from Troms, northern Norway. Lithos, 5, 345–364.

Schreyer, Werner, Abraham, Kurt, and Kulke, H.H.G. (1980) Natural sodium phlogopite coexisting with potassium phlogopite and sodian aluminian talc in a metamorphic evaporite sequence from Derrag, Tell Atlas, Algeria. Contributions to Mineralogy and Petrology, 74, 223–233.

Schreyer, Werner, Horrocks, P.C., and Abraham, K. (1984) High-magnesium staurolite in a sapphirine-garnet rock from the Limpopo Belt, Southern Africa. Contributions to Mineralogy and Petrology, 86, 200–207.

Seifert, Fritz. (1975) Boron-free kornerupine: A high-pressure phase. American Journal of Science, 275, 57–87.

Vrána, S., and Barr, M.W.C. (1972) Talc-kyanite-quartz schists and other high-pressure assemblages from Zambia. Mineralogical Magazine, 38, 837–846.

Waters, D.J., and Moore, J.M. (1985) Kornerupine in Mg–Al-rich gneisses from Namaqualand, South Africa: Mineralogy and evidence for late-metamorphic fluid activity. Contributions to Mineralogy and Petrology, 91, 369–382.

Werding, Gunther, and Schreyer, Werner. (1978) Synthesis and crystal chemistry of kornerupine in the system $MgO-Al_2O_3-SiO_2-B_2O_3-H_2O$. Contributions to Mineralogy and Petrology, 67, 247–259.

Williams, H.R. (1984) Field relations and chemistry of sapphirine-bearing rocks from the Bjørnesund area, Fiskenaesset, western Greenland. Canadian Mineralogist, 22, 417–421.

Yefimov, I.A. (1967) Mestorozhdeniye lyapis-lazuri Sary-Sang v Severnom Afganistane (The lapis-lazuli deposit of Sar-e-Sang in northern Afghanistan). Vestnik Akademii Nauk Kazakhskoy SSR, 8, 64–66 (in Russian).

Yurgenson, G.A., and Sukharev, B.P. (1984) Usloviya lokalizatsii i mineralnaya zonalnost lazuritonosnykh tel Badakhshana. Zapiski Vsesoyuznogo Mineralogicheskogo Obshchestva, 113(4), 498–505 (English translation: Localization of lapis lazuli bodies of Badakhshan and their mineral zonation. International Geology Review, 27, 230–237, 1985).

Zen, E-an. (1963) Components, phases, and criteria of chemical equilibrium in rocks. American Journal of Science, 261, 929–942.

Zotov, I.A. (1968) Nekotoryye osobennosti magmatisma i metamorfizma kristallicheskogo kompleksa yugo-zapadnogo Pamira (Several features of the magmatism and metamorphism of the crystalline complex of the southwestern Pamirs). In avtoreferaty rabot sotrudnikov Instituta Geologii Rudnykh Mestorozhdeniy, Petrografii, Mineralogii i Geokhimii Akademii Nauk SSSR za 1967 gody.